FDTD Simulation of a Cylindrical Waveguide Using Longitudinal Current Distribution as an Excitation Scheme

D. V. Peponis, G. P. Latsas, Z. C. Ioannidis, and I. G. Tigelis
Faculty of Physics, National and Kapodistrian University of Athens
University Campus, Athens 157 84, Greece

Abstract— In this work we present a numerical code based on the FDTD method in the cylindrical coordinate system. In order to verify the code, the simple case of a cylindrical waveguide excited by an axial current distribution is considered. The waveguide is terminated using two CFS-PML layers in order to eliminate reflections at both ends.

1. INTRODUCTION

Recently, the demand for high-power and high-frequency microwave sources have led to the development of sophisticated microwave structures. Due to their complexity, the analytical study of those is difficult and thus numerical techniques are usually employed, one of them being the FDTD method. Such techniques often use Cartesian grids, in which obviously cylindrical structures cannot be accurately modelled. Specifically, the curvatures in these structures are approximated by a staircase scheme, which introduces undesired errors [1]. To overcome these problems, FDTD codes in cylindrical coordinates have been developed in the past based on an appropriately modified Yee algorithm, primarily used in low frequency problems [2–4]. In this work, the FDTD method (and the corresponding developed numerical code) in cylindrical coordinate system formulated for studying complex cylindrical geometries appearing in high-frequency devices (like the gyrotron beam tunnel), is used for the simple case of a smooth waveguide. The Maxwell equations are written appropriately in order to eliminate the aforementioned conformal problems [1, 6]. Moreover, a CFS-PML layer [7] is used for the termination of the waveguide. As an excitation scheme, an infinitely thin wire is considered, located on the propagation axis, with a predefined current density. This type of excitation could model the case of the excitation of the waveguide modes by a thin electron beam in such a waveguide structure in the small signal regime. In this study, only the dominant TM_{01} mode is excited due to the choice of frequency range. Finally the effect of the CFS-PML on the reflection at both ends of the structure is studied in the whole frequency range under investigation.

2. MATHEMATICAL FORMULATION OF THE METHOD

The discretized Maxwell equations in Cylindrical coordinates are written appropriately taking into account the source term J, i.e., the radial component of the electric field, E_ρ, is:

$$\begin{aligned} E_\rho|^{n+1}_{i+1/2,j,k} =\ & \frac{2\varepsilon|_{i+1/2,j,k} - \sigma|_{i+1/2,j,k}\delta t}{2\varepsilon|_{i+1/2,j,k} + \sigma|_{i+1/2,j,k}\delta t} E_\rho|^{n}_{i+1/2,j,k} + \frac{2\delta t}{2\varepsilon|_{i+1/2,j,k} + \sigma|_{i+1/2,j,k}\delta t}\Bigg[-J_\rho|^{n+1/2}_{i+1/2,j,k} \\ & + \frac{H_z|^{n+1/2}_{i+1/2,j+1/2,k} - H_z|^{n+1/2}_{i+1/2,j-1/2,k}}{(i+1/2)\,\delta\rho\delta\varphi} - \frac{H_\varphi|^{n+1/2}_{i+1/2,j,k+1/2} - H_\varphi|^{n+1/2}_{i+1/2,j,k-1/2}}{\delta z}\Bigg] \end{aligned} \tag{1}$$

where δt is the timestep, $\delta\rho$, $\delta\varphi$ and δz are the mesh spatial increments in ρ, φ and z directions, respectively, σ the conductivity and ε the dielectric permittivity of the medium inside the waveguide. Indexes i, j and k refer to the grid position in ρ, φ and z directions, respectively. All the field components are properly located within the cylindrical Yee cell, which is shown in Fig. 1, in order for Ampere and Faraday laws to be valid.

The analytical field equations of Ampere and Faraday laws present a singularity at $\rho = 0$ for E_z and H_ρ time derivatives [2], and this problem appears in the discretized expressions as well. On the other hand, E_φ cannot be properly calculated at $\rho = 0$ due to the need for field values at $i = -1/2$, which are not defined. These problems can be overcome with the proper application of Ampere law at the neighbouring grid points, as presented in [2].

In order to eliminate the reflections at the terminations of the waveguide, two CFS-PML layers were used, one at each end (Fig. 2). These layers were implemented using the stretched coordinates

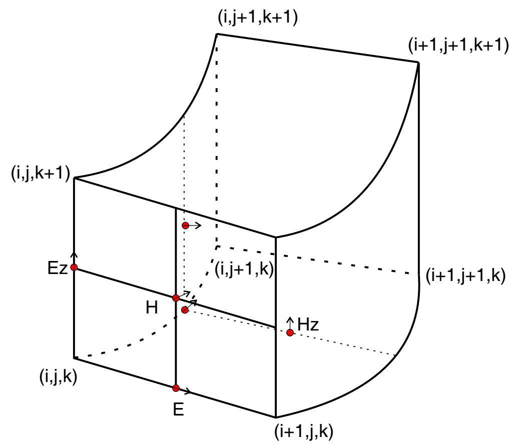

Figure 1: Cylindrical Yee cell.

formulation [7]. Coordinate stretching was applied only in the direction perpendicular to the interface of the PML-structure [8], i.e., the z-axis. The scaling characteristics of CFS-PML layer were calculated with respect to the cutoff frequency of the modes expected to excite in the structure. In detail, the complex conductivity tensor of the layer is given by [9]

$$s_i = k_i + \frac{\sigma_i}{\alpha_i + j\omega\varepsilon_0},\ i = \rho, \varphi, z \tag{2}$$

where s_i is the CFS-PML layer's conductivity, ω the angular velocity and ε the layer's electric permittivity. The maximum value of the a_i term can be chosen taking into account the cutoff frequencies of the expected modes. In the case, where only one mode is present, it is given by [8]

$$\alpha_{i,max} = 2\pi f_c \epsilon_0,\ i = \rho, \varphi, z \tag{3}$$

where f_c is the cutoff frequency of the selected mode. The conductivity σ_i, which appears in the stretching factor, can follow either a polynomial or a geometrical profile on the axis where stretching is applied. For a polynomial profile, the maximum value of the conductivity is given by [6]

$$\sigma_{i,max} = -\frac{(m+1)ln[R(0)]}{2\eta d},\ i = \rho, \varphi, z \tag{4}$$

where m is the polynomial factor, $R(0)$ the desired reflection coefficient of the layer for normal incidence, η the layer impedance and d its thickness.

3. NUMERICAL RESULTS AND DISCUSSION

In order to verify the applied method and to benchmark the numerical code, the simple case of a smooth hollow cylindrical waveguide was examined, with the excitation implemented by an infinitely thin wire of specific current density located at the axis of the waveguide. The axial cross section is shown in Fig. 2 whereas the geometrical characteristics are given in Table 1. The current density is spatially constant, whereas in time it varies as a Gaussian modulated sinusoid with predefined spectral characteristics. Its frequency content is such that only TM_{01} mode (with $f_c = 8.19\,\mathrm{GHz}$) can be propagated. The central frequency of the pulse is $f_0 = 9\,\mathrm{GHz}$ and the Full Width at Half Maximum (FWHM) is $FWHM = 470\,\mathrm{MHz}$. The total duration of the excitation signal is 30 ns. A field monitor (where temporal field values are recorded) is placed at $(\varrho, \varphi, z) = (0\,\mathrm{mm}, 0, 20\,\mathrm{mm})$ in order to be far enough from the current source and the field values to be maximum in the radial direction.

Table 1: Geometrical characteristics of the simulated waveguide.

Length L (mm)	**Radius α (mm)**	**Current wire length L_{curr} (mm)**	**PML thickness (cells)**
400	14	2	10

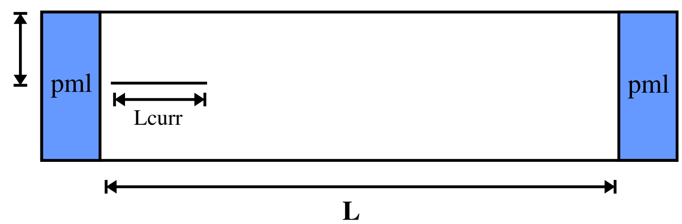

Figure 2: Axial cross section of the simulated waveguide (not in scale).

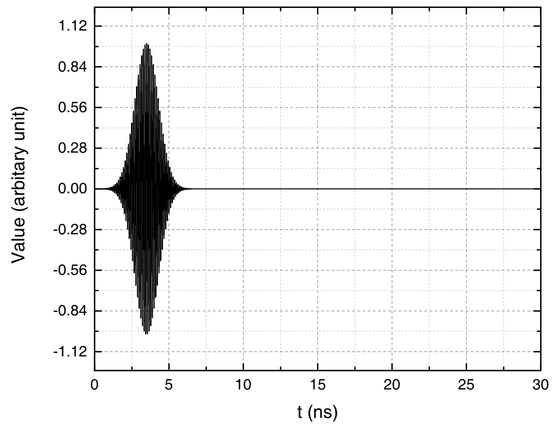

Figure 3: Excitation signal.

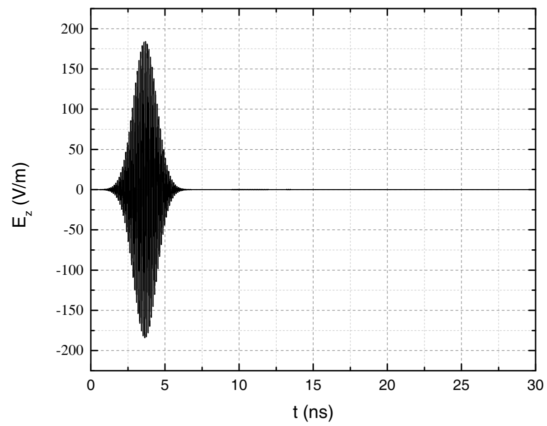

Figure 4: E_z component at $(\rho, \varphi, z) = (0, \frac{\pi}{2}, 20)$.

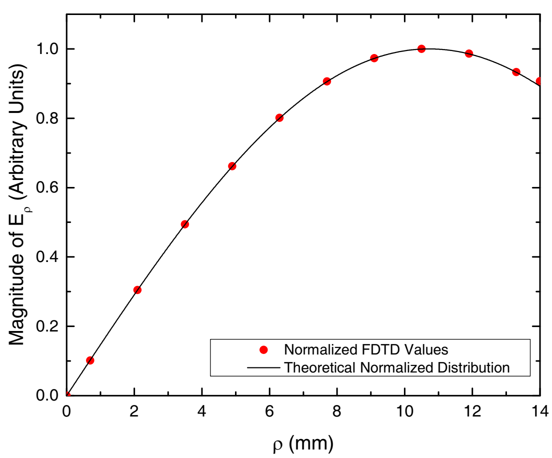

Figure 5: Radial distribution of normalized E_ρ component for $t = 3.5$ ns.

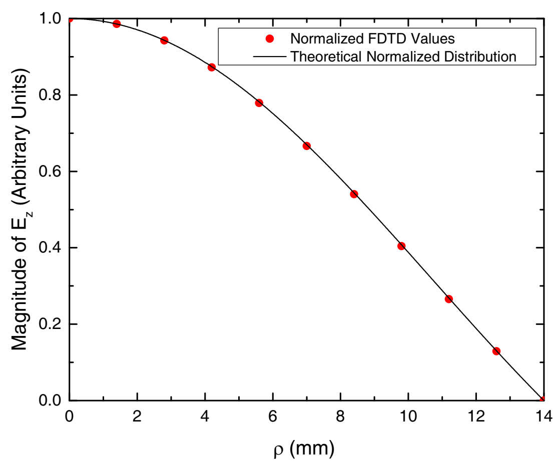

Figure 6: Radial distribution of normalized E_z component for $t = 3.5$ ns.

The time driving function is shown in Fig. 3, while the signal output of E_z, at $(\rho, \varphi, z) = (0, \frac{\pi}{2}, 20)$ is shown in Fig. 4[1]. From this figure only the travelling pulse appears and therefore there is no reflection from the CFS-PML regions, leading to a macroscopical behaviour of an infinite waveguide.

The normalized radial distributions of E_ρ and E_z at $(\varphi, z) = (\frac{\pi}{2}, 20)$ are given in Fig. 5 and Fig. 6, respectively. In the same figures the values of normalized field components obtained by the theoretical analytical expressions $E_\rho \propto J'_m(k_c\rho)$ and $E_z \propto J_m(k_c\rho)$ are also plotted, where k_c is the cutoff wavenumber for the mode TM_{mn}. The values at positions where no grid points are defined, were calculated using the Richardson extrapolation method [10]. The 2D distributions for the same components are given in Fig. 7 for E_ρ and in Fig. 8 for E_z. Both radial distributions and two dimensional distributions on the $\rho - \varphi$ plane follow the theoretically expected ones of the TM_{01} mode, therefore it is evident that only this mode is excited and propagates in the waveguide.

The effect of the absence of the CFS-PML is shown in Fig. 9. The signal at the position

[1]Note that the thickness of the line and the high frequency leads to a dense plot and does not allow the signals to be clearly plotted properly and thus they appear as black regions with a specific envelope function, representing the pulse function.

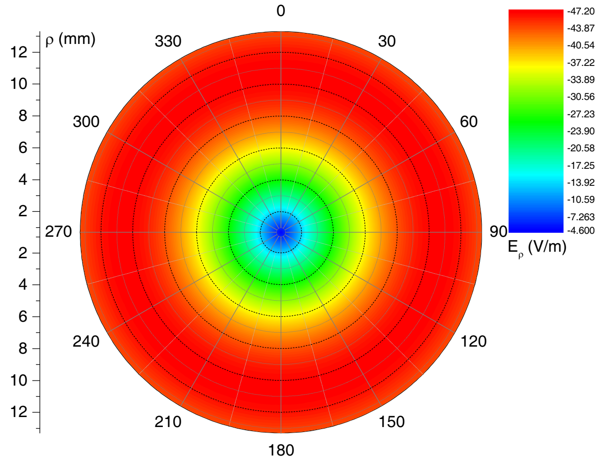

Figure 7: E_ρ distribution on $\rho - \varphi$ plane for $t = 3.5\,\mathrm{ns}$.

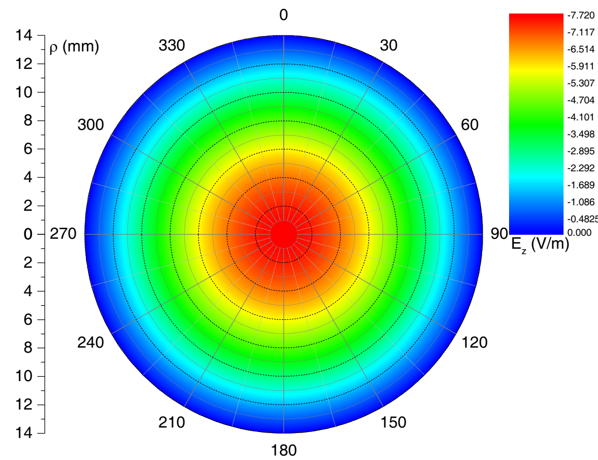

Figure 8: E_z distribution on $\rho - \varphi$ plane for $t = 3.5\,\mathrm{ns}$.

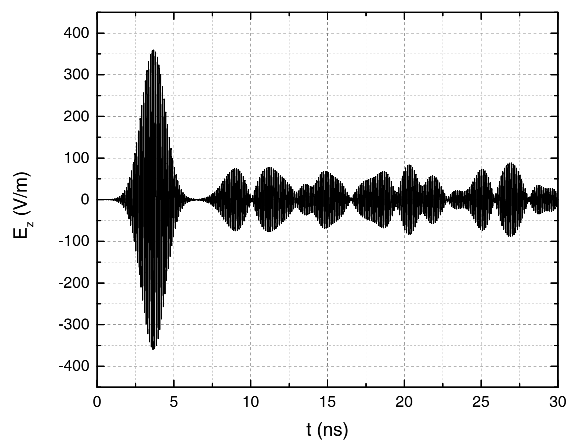

Figure 9: E_z at $(\rho, \varphi, z) = (0, \frac{\pi}{2}, 20)$ in a short-circuit ended waveguide.

$z = 20\,\mathrm{mm}$ is a combination of the incident and the reflected waves originated from the two waveguide ends which are now short-circuited (PEC boundary condition). This means that the waveguide behaves now like a cylindrical cavity. Comparing the result in Fig. 9 with the one of Fig. 4 it is clear that the use of a precisely tuned CFS-PML layer in a FDTD simulation of a waveguide results in the total absorption of the incident waves at the ends.

4. CONCLUSIONS

A smooth hollow cylindrical waveguide was studied using using a numerical code developed in C and based on the FDTD method in cylindrical coordinate system with an infinitely thin wire with a constant current density as an excitation scheme. The advantage of this method is the inherit conformity to cylindrical structures. The introduction of current terms in the discretized expressions gives the flexibility to model virtually any current distribution, whose the spatial, spectral and time characteristics are defined explicitly by the user. Possible application of the presented numerical code is the simulation of a complex cylindrical structure excited by an electron beam in the small signal regime, like the gyrotron beam tunnel, cavity etc. Finally, the precise tuning of the CFS-PML layer characteristics can lead to a full absorption resulting to a more accurate simulation of the behaviour of a perfectly matched waveguide.

ACKNOWLEDGMENT

This work has been carried out within the framework of the EUROfusion Consortium and has received funding from the Euratom research and training programme 2014-2018 under grant agreement No 633053 (WPEDU). The views and opinions expressed herein do not necessarily reflect those of the European Commission.

REFERENCES

1. Harms, P. H., J.-F. Lee, and R. Mittra, "A study of the nonorthogonal FDTD method versus the conventional fdtd technique for computing resonant frequencies of cylindrical cavities," *IEEE Transactions on Microwave Theory and Techniques*, Vol. 40, No. 4, 741–746, 1992.
2. Chi, J., F. Liu, L. Xia, T. Shao, and S. Crozier, "An improved ccylindrical FDTD algorithm and its application to field-tissue interaction study in MRI," *IEEE Transactions on Magnetics*, Vol. 47, No. 2, 466–470, 2011.
3. Liu, F. and S. Crozier, "An FDTD model for calculation of gradient-induced eddy currents in MRI system," *IEEE Transactions on Applied Superconductivity*, Vol. 14, No. 3, 1983–1989, 2004.
4. Trakic, A., H. Wang, F. Liu, H. Sanchez Lopez, and S. Crozier, "Cylindrical 3D FDTD algorithm for the computation of low frequency transient eddy currents in MRI," *ISMRM 14th Scientific Meeting* & *Exhibition*, Vol. 1, No. 1, 1373–1373, International Society for Magentic Resonance in Medicine (ISMRM), 2006.
5. Yee, K. S.,et al., "Numerical solution of initial boundary value problems involving Maxwell's equations in isotropic media," *IEEE Transactions on Antennas and Propagation*, Vol. 14, No. 3, 302–307, 1966.
6. Taflove, A. and S. C. Hagness, *Computational Electrodynamics*, Artech House, 2005.
7. Roden, J. A. and S. D. Gedney, "Convolutional PML (CPML): An efficient FDTD implementation of the CFS-PML for arbitrary media," *Microwave and Optical Technology Letters*, Vol. 27, No. 5, 334–338, 2000.
8. Berenger, J.-P., "Perfectly Matched Layer (PML) for computational electromagnetics," *Synthesis Lectures on Computational Electromagnetics*, Vol. 2, No. 1, 1–117, 2007.
9. Inan, U. S. and R. A. Marshall, *Numerical Electromagnetics: The FDTD Method*, Cambridge University Press, 2011.
10. Cheney, E. and D. Kincaid, *Numerical Mathematics and Computing*, Cengage Learning, 2012.